

AD-A136 627

PERFORMANCE COMPARISON OF A HYDRAULIC BREAKWATER  
ATTENUATING RANDOM AND MONOCHROMATIC WAVES(U) NAVAL  
POSTGRADUATE SCHOOL MONTEREY CA D G BASILE DEC 83

1/1

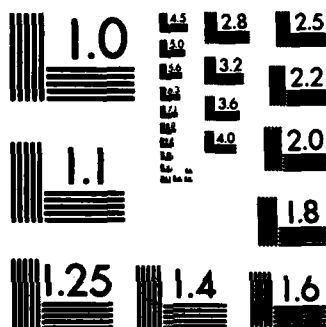
UNCLASSIFIED

F/G 13/2

NL



END



MICROCOPY RESOLUTION TEST CHART  
NATIONAL BUREAU OF STANDARDS-1963-A

A136627

PERFORMANCE COMPARISON OF A HYDRAULIC  
BREAKWATER ATTENUATING RANDOM AND  
MONOCHROMATIC WAVES

by  
David T. Basile

ON 605 REPORT  
Submitted to Dr. J. B. Herbich  
Texas A&M University

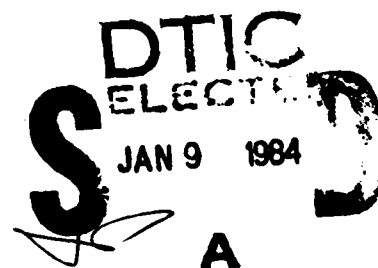
Copy available to DTIC does not  
permit fully legible reproduction

In partial fulfillment  
of the requirements for the  
degree of  
Master of Engineering

Naval Postgraduate School  
Monterey, CA 93940

December 1983

This document has been approved  
for public release and sale; its  
distribution is unlimited.



DTIC FILE COPY

84 01 09 014

## **DISCLAIMER NOTICE**

**THIS DOCUMENT IS BEST QUALITY  
PRACTICABLE. THE COPY FURNISHED  
TO DTIC CONTAINED A SIGNIFICANT  
NUMBER OF PAGES WHICH DO NOT  
REPRODUCE LEGIBLY.**

## ABSTRACT

Based on work performed by various engineers and scientists, (Straub, et al; Taylor; Williams; Horikawa; etc.), small scale experiments were performed to compare the performance of a hydraulic breakwater for attenuation of various random wave spectra to monochromatic waves. Previous experiments were conducted in the presence of monochromatic waves and wind generated waves, the wind generated waves being closer to natural occurrences than monochromatic waves.

Four wave spectra, Darbyshire, Pierson, ITTC and Jonswap, were generated against a breakwater set at a fixed depth and fixed jet area per foot (maximum mechanically attainable) while varying the flowrate.

The results indicate a much larger discharge requirement for the attenuation of random waves to the same degree as monochromatic waves of similar magnitude. This is due to the fact that the breakwater does not work as well on the longer waves of the spectrum as it does on the shorter waves.



Per Form 50	
Classification/	
Availability Codes	
Present and/or	
Special	
A-1	23 GP

## TABLE OF CONTENTS

	Page
Abstract	2
List of Tables and Figures	4
List of Symbols	5
Introduction	7
Discussion of Data	11
Apparatus	12
Experimental Results	14
Conclusions	16
Tables and Figures	17
References	24

## LIST OF TABLES AND FIGURES

	Page
Table 1	18
Summary of Experimental Results	
Table 2	19
Standard Empirical Spectra	
Figure 1	20
Sample Random Wave Strip Chart	
Figure 2	21
Experimental Apparatus Set-up	
Figure 3	22
Breakwater Manifold	
Figure 4	23
Graph of Attenuation to Unit Discharge for Experimental Results	

## LIST OF SYMBOLS

$a$	=	boundary condition constant
$a_c$	=	channel cross-sectional area
$a_j$	=	cumulative jet area
$b$	=	boundary condition constant
$B_1$	=	initial condition constant
$B_2$	=	initial condition constant
$C$	=	initial condition constant
$d$	=	water depth
$Fr$	=	Froude Number
$g$	=	gravitational acceleration constant
$h$	=	depth of jet-induced current
$H_{AVG}$	=	average incident wave height
$H_{MAX}$	=	maximum incident wave height
$H_{SIG}$	=	significant incident wave height
$H_{TSIG}$	=	significant transmitted wave height
$k$	=	wave number (integer)
$L$	=	wave length of transmitted wave
$L_0$	=	wave length of incident wave
$q$	=	discharge per foot of breakwater
$Q$	=	total discharge of breakwater
$t$	=	time
$T$	=	wave period
$T_p$	=	peak wave period of wave spectrum



$V$  = mean velocity from water jets and surface current

$x$  = horizontal space coordinate

$y$  = vertical space coordinate

$Z_2$  = Taylor's non-dimensional coefficient relating  
wave length to surface current parameters

$\phi_1$  = surface current velocity potential

$\phi_2$  = velocity potential below surface current

## INTRODUCTION

Wave attenuation by surface currents created by pneumatic and hydraulic breakwaters has been studied for many years. Studies of pneumatic breakwaters will not be discussed, except to say the early research of hydraulic breakwaters was directly related to the pneumatic breakwater experimental results, ie, the horizontal current set up near the water surface by the rising bubbles was the main cause for wave attenuation, as is the case of the current set up by the horizontal water jets. The major motivation for the development of hydraulic breakwaters was to develop a transportable, easily erected and operated breakwater to expedite emergency operations, such as oil spill clean up or salvage. The breakwater could be stowed on a vessel, installed where needed and operated by pumps already installed on the ships. Another application would be to use the breakwater during off-shore or coastal construction, such as bridge, pier and platform construction, where no breakwater existed before or would be needed after construction was completed. There are also various military applications.

A hydraulic breakwater is formed by discharging water under pressure through a series of orifices or nozzles in a manifold in a direction opposite to incident waves. As the water jets from the breakwater interact with the surrounding water, a high degree of turbulence is generated. This turbulence and diffusion eventually create a horizontal current. When waves enter this current, part of their energy is dissipated. As a result of this energy loss, the height of the transmitted waves beyond the breakwater is less than that of the incident waves, with 100% attenuation as a goal.

Hydraulic breakwaters were heavily studied in the mid to late 1950's. Taylor<sup>1</sup> manipulated mathematical equations for two surface current profiles, one constant with depth, the other linearly decreasing with depth, for 100% wave attenuation. He showed the relationship between horizontal current velocity and attenuation of incoming waves. Experimental results have shown that the linearly decreasing velocity profile is a close approximation. For this current, he represents waves, of wave length  $L = 2\pi/k$  and frequency  $T/2\pi$ , by velocity potentials  $\phi_1$  on the surface current and  $\phi_2$  below the current:

$$\begin{aligned}\phi_1 &= -V_x + (B_1 e^{ky} + B_2 e^{-ky}) e^{i(kx - Tt)} \\ \phi_2 &= C e^{k(y+h)} e^{i(kx - Tt)}\end{aligned}$$

if the surface wave is  $y = a e^{i(kx - Tt)}$  and the lower surface is  $y = -h + b e^{i(kx - Tt)}$  ( $k > 0$ ). He then non-dimensionalizes these equations and finds the relationship:

$$Z_2 = 2\pi h \alpha_2^2 / L_0 = hg / V_2^2$$

with  $h$  = depth of current,  $L_0$  = wavelength of incident waves,  $g$  = gravitational acceleration,  $V_2$  = velocity needed to completely attenuate the waves and  $\alpha_2$  is a coefficient defined as  $g/VT$ ,  $T$  = wave period. He tabulates values of  $\alpha_2$  as a function of  $L_0/2\pi h = \alpha_2^2 / Z_2$  in Table 4.

As an example,  $L_0 = 5$  ft.,  $k=1$ ,  $h=5$  in., then  $L_0/2\pi h = 1.91$ , and from Table 4,  $-\alpha_2 = 2.60$  then,  $2\pi h \alpha_2^2 / L_0 = 3.54 = hg/V_2^2$ , and  $V_2 = 1.95$  fps. An approximate flow rate through the jets necessary to create the required velocity can be calculated if the area of the current-creating jets is known. Say  $a_j = .005$  sf. Then,  $Q = V_2 a_j = .01$  cfs is needed to attenuate the waves.

Evans<sup>2</sup> performed model studies showing the importance of the surface current generated by the breakwater's jets. He states and shows that waves may be stopped by a sufficiently thick opposing surface current and that the period of the waves remains unchanged as they pass into the current. His experiments showed that waves will be at least partially damped by the turbulent action caused by a counter-current. Evans' tests were for shallow water conditions, where as Taylor's equations are for infinitely deep water.

Straub, et al,<sup>3,6</sup> performed two separate scale experiments to determine scale effects and horsepower requirements for efficient operation of hydraulic breakwaters. As test parameters, they varied jet area per foot of breakwater, jet angle of attack, jet depth per water depth, jet discharge and number of jet nozzle manifolds. Their data are presented in dimensional and non-dimensional form. It was determined that the scaling factor is the Froude Number,  $Fr^2 = V^2/gd = \text{constant}$ , jet depth for best results is .91 water depth from the bottom, so as to stay below the wave troughs, and jet area per foot of breakwater should be maximized.

Using the example from above, wave length  $L_0 = 5$  ft, depth  $d = 2$  ft, jet area  $a_j = .01$  sf and graphs from Straub, et al,

$$L_0 / d = 2.5$$

jet submergence = 21.4 inches from the bottom. From their Fig. 5, discharge per foot of breakwater  $q = .018$  cfs for 90% attenuation of the waves. And from their Fig. 8, for 100% attenuation,  $q = .018$  cfs. Horsepower and discharge requirements as functions of  $a_j$  are found in their Fig. 6 in dimensionless form.

Other studies were conducted, notably three-dimensional studies by Straub, et al<sup>3</sup> and Horikawa,<sup>5</sup> to determine the area of protection behind breakwaters that are set at various angles to the attacking incident wave trains; a breakwater installed aboard a ship (Dilley<sup>4</sup>) to protect the ship and mooring system during operations in deep water; the verification of the Froude Number as the scaling factor (Williams<sup>7</sup>), as gravity forces on the free water surface play an important role in the attenuation process; and attenuation of wind waves (Williams and Wiegel<sup>8</sup>) the closest to natural phenomena. It was determined that longer, deeper waves were not attenuated as effectively as the shorter, shallower waves. Rao<sup>9</sup> and Rhee, Richey and Rao<sup>10</sup> updated and reverified previously collected data for deep water waves. It was determined by these experiments that horsepower requirements might be less than previously expected, but further studies would have to be performed.

Most previous experiments were conducted using monochromatic waves. It will be attempted to show a very limited case of the hydraulic breakwater, with fixed jet area, fixed jet angle and fixed jet submergence. Various random wave spectra attenuation will be compared to Straub, et al<sup>3</sup>, results as to efficiency of the hydraulic breakwater. The wave spectra used were Darbyshire, ITTC, Jonswap and Pierson-Moskowitz, as these were library spectra installed in the wave generator system. Table 2 shows the equations used to describe the various wave spectra. A sample of the strip chart generated by the ITTC spectrum at  $q = .03$  cfs/ft is shown in fig. 1.

## DISCUSSION ON JETS

A basic axiom<sup>11</sup> of jet hydraulics states that the entire kinetic energy of a jet will be dissipated through reaction with the surrounding fluid. And the Newtonian principle of action and reaction makes it plain that deceleration of the fluid in the jet, caused by turbulent diffusion, occurs through simultaneous acceleration of the surrounding fluid. The prediction of the surface velocity and thickness of the surface current from the discharge of the water jets is an essential factor in the practical use of hydraulic breakwaters.

A way of predicting the jet's velocity profile is given by Albertson, et al<sup>11</sup>. He gives expressions for both slots and circular orifices. For a slot width equal to orifice diameter, and all other parameters equal, the maximum slot velocity is less than the maximum orifice velocity, both measured on the centerline, respectively. Albertson, et al, present various non-dimensional plots of velocity profile parameters for the use of engineers and designers. Jen, et al<sup>12</sup>, bring in the effects of temperature, but in the experiments reported on in this paper, these effects are neglected.

## APPARATUS

The experimental apparatus consists of a wave tank, wave generator and hydraulic breakwater. The tank is a 120 ft long, 24.5 inch wide, two-dimensional glass walled flume. The wave generator is located at the head of the tank, while a wave absorbing beach is at the end. Water depth was kept constant at 20 inches (fig. 2). The channel area,  $a_c = (24.5)(20)/144 = 3.403$  sq. ft.

The jet size and manifold placement were approximated using Straub, et al, results. The breakwater consists of a 1.5 inch I.D. PVC pipe manifold fed through a central Tee junction by a pump rated at 80 gpm through a 1.5 inch I.D. pipe (fig. 3). The breakwater manifold is secured at a fixed height from the bottom of the tank<sup>3</sup>, 18.25 inches (.91 depth). The manifold has twenty-two 7/32 inch brass nozzle jets spaced 1 inch apart center to center, for a total jet area  $a_j = .827$  sqin. The jet area was set so as to be maximum mechanically possible. This gave a jet area to channel area ratio of .00169.

The wave generator is a Seasim Modular Wave Making system, consisting of a Seasim Programmable Spectrum Random Signal Generator, a Rolling Seal Wave Maker RSW 30-60, and a Servo Control Amplifier LSC 24-48. The breakwater was set into the tank 45 ft from the wave generator, with two resistance-type wave gages, one 20 ft ahead and one 20 ft behind the breakwater (fig. 2).

To determine the maximum discharge requirement, and from this the pump size necessary, Straub, et al<sup>3</sup>, Fig. 8. was used. A maximum flow rate per foot of breakwater  $q = .025$  cfs/ft was chosen, since 100% attenuation of wave lengths used in this experiment occurred before this value was reached. Thus, an estimated  $Q = (.025)(2.04) = .051$  cfs = 22.5 gpm was needed at the nozzles of the

breakwater. It was thought that the University's water supply would be sufficient to deliver the required flow rate, but after preliminary tests was determined unacceptable. The laboratory pump used was rated at 80 gpm through a 1.5 inch pipe. Water was fed to the pump directly from the tank, the suction end far away from the experimental apparatus, so the water level in the tank would remain essentially constant. An orifice meter was installed in the pump outlet line and attached to a mercury manometer to be able to accurately measure the flow rate from the pump to the breakwater.



## WIND-INDUCED WAVES

In all the tests performed, the attenuation of all the waves was of the same order of magnitude. This is probably due to the fact that the manifold is made of large diameter pipes, and therefore the shorter, steeper waves were attenuated more than the longer waves virtually to the point of disappearance of the transmitted spectrum. The attenuation increased approximately 15 percent for the waves which were attenuated just to the point of disappearance.

The wave lengths and periods were given by

$$L_p = \frac{g}{2\pi} T_p^2$$

$T_p$  = peak wave period,  $L_p$  = wave length,  $d$  = water depth and  $L_p$  = wave length corresponding to peak period of the incident wave. Since the maximum attenuation was not attained, comparisons with the work of et al, horsepower and efficiency, could not be made. However, attenuation comparisons can be made with data and the various wave spectra were taken and are shown in figure 4.

Figure 4 shows an attenuation of approximately .28 for no discharge. This was because the manifold itself acted as a wave absorber, the manifold diameter being of the same order of magnitude as the wave heights and situated close to the water surface. The ratio of the manifold diameter to the wave height in these experiments was greater than that used by Straub, et al, hence the difference in results.

The most striking difference between the broadband and monochromatic wave attenuation is that the broadband

to discharge is increasing at a much slower rate for random waves than for monochromatic waves. This would lead one to believe it requires more discharge, and therefore more power, per foot of breakwater to attain the same degree of attenuation of random waves of the same significant period and height as the period and height of a monochromatic wave train, with the same breakwater.

The attenuation of each different spectrum was calculated for each of average wave height, significant wave height and maximum wave height. These were calculated using a fast Fourier transform (smoothed periodogram) computer program written at Texas A&M University. In all cases, the same amount of attenuation was achieved, so only the significant wave heights of the transmitted waves were tabulated in Table 1. The significant wave height was chosen as this is normally chosen as the design wave for most applications.

It was noted that the water in front of the breakwater rose slightly at high rates of discharge, except directly in front of the breakwater. The velocity of the water jets caused the surrounding water to be pulled away from the breakwater, by the interactive forces discussed above, at a higher rate than the water behind the breakwater could naturally fill the void. No solution to this problem, if it is a problem, will be put forward.

## CONCLUSIONS

1. The rate of attenuation for the random wave spectra tested is less than comparable monochromatic waves, by approximately a factor of 2.
2. Using the above as a guide, horsepower and efficiency comparisons would most probably be affected in a similar manner.
3. The shorter waves of the spectra were attenuated out by the breakwater, but the longer waves continued through virtually unaffected.
4. Comparison of attenuation of average, significant and maximum wave heights showed they were equal.

TABLES  
AND  
FIGURES

TABLE 1. SUMMARY OF EXPERIMENTAL RESULTS

Darbyshire Spectrum		$T_p = .98s$	$L_0/d = 3.63$
$H_{SIG} = 1.29$ in	$H_{AVE} = .81$ in	$H_{MAX} = 1.65$ in	
$q(cfs/ft)$	$H_{TSIG}(in)$	Attenuation	$T_p(sec)$
0	.98	.34	1.16
.018	.92	.37	1.16
.029	.80	.38	1.16
.041	.67	.45	1.16
Pierson-Moskowitz Spectrum		$T_p = .91s$	$L_0/d = 3.27$
$H_{SIG} = 1.37$ in	$H_{AVE} = .86$ in	$H_{MAX} = 1.74$ in	
$q(cfs/ft)$	$H_{TSIG}(in)$	Attenuation	$T_p(sec)$
0	1.01	.26	.98
.020	.89	.35	1.16
.028	.78	.43	1.16
.047	.60	.56	1.28
ITTC Spectrum		$T_p = .98s$	$L_0/d = 3.63$
$H_{SIG} = 1.43$ in	$H_{AVE} = .89$ in	$H_{MAX} = 1.82$ in	
$q(cfs/ft)$	$H_{TSIG}(in)$	Attenuation	$T_p(sec)$
0	.93	.35	1.16
.018	.88	.38	1.16
.030	.70	.51	1.16
.042	.56	.61	1.28
Jonswap Spectrum		$T_p = .98s$	$L_0/d = 3.63$
$H_{SIG} = 1.43$ in	$H_{AVE} = .98$ in	$H_{MAX} = 1.82$ in	
$q(cfs/ft)$	$H_{TSIG}(in)$	Attenuation	$T_p(sec)$
0	1.02	.29	1.16
.017	.96	.33	1.16
.028	.85	.41	1.16
.036	.72	.50	1.16

TABLE 2 STANDARD EMPIRICAL SPECTRA

Darbyshire Coastal Water Spectrum

$$S(f) = 1.494 \gamma H_S^2 \exp \left\langle \frac{\gamma^2 (f - f_0)^2}{0.0085 (f - f_0)^2 + 0.042} \right\rangle$$

where  $f_0 = 1/T_0$

Pierson Moskowitz Spectrum

$$S(f) = Af^{-2} \exp \left\langle -Bf^{-4} \right\rangle$$

where  $A = 0.0795 H_S^2 / T_1^4$

$$B = 0.3183 / T_2^4$$

ITTC Spectrum

$$S(f) = Af^{-5} \exp \left\langle -Bf^{-4} \right\rangle$$

where  $A = 0.111 H_S^2 / T_1^4$

$$B = 0.443 / T_1^4$$

Jonswap Spectrum

$$S(f) = Af^{-5} \exp \left\langle -\frac{5}{4} \left( \frac{f_0}{f} \right)^4 \right\rangle \gamma^B$$

where  $A = 603.9 \frac{H_S^2 f_0^2}{g}^{2.036} (1 - 0.298 \log \gamma) 0.06171$

$$B = \exp \left\langle -\frac{(f - f_0)^2}{2 \sigma^2 f_0^2} \right\rangle$$

$\sigma = 0.07$  if  $f \leq f_0$   
 $\sigma = 0.09$  if  $f > f_0$  and  $f_0 = 1/T_0$

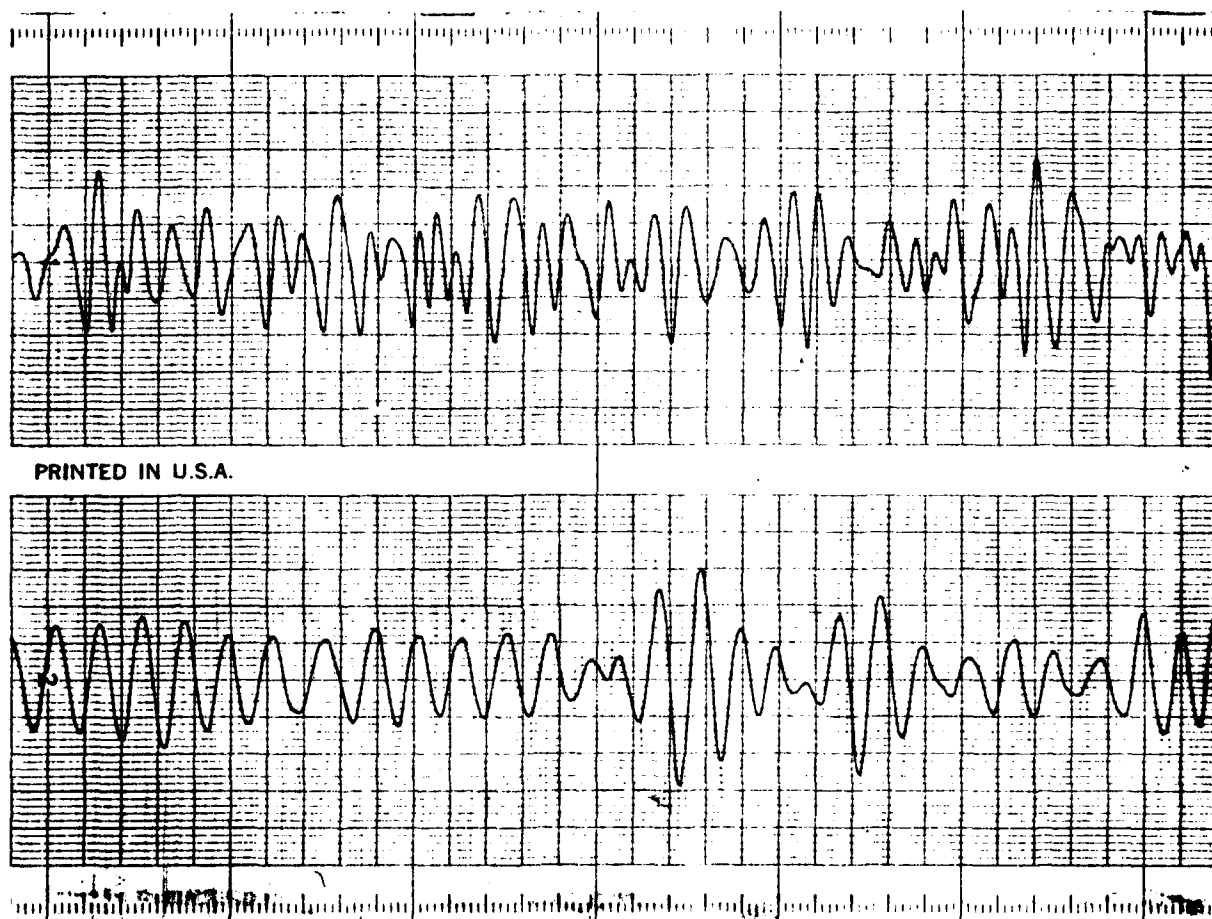
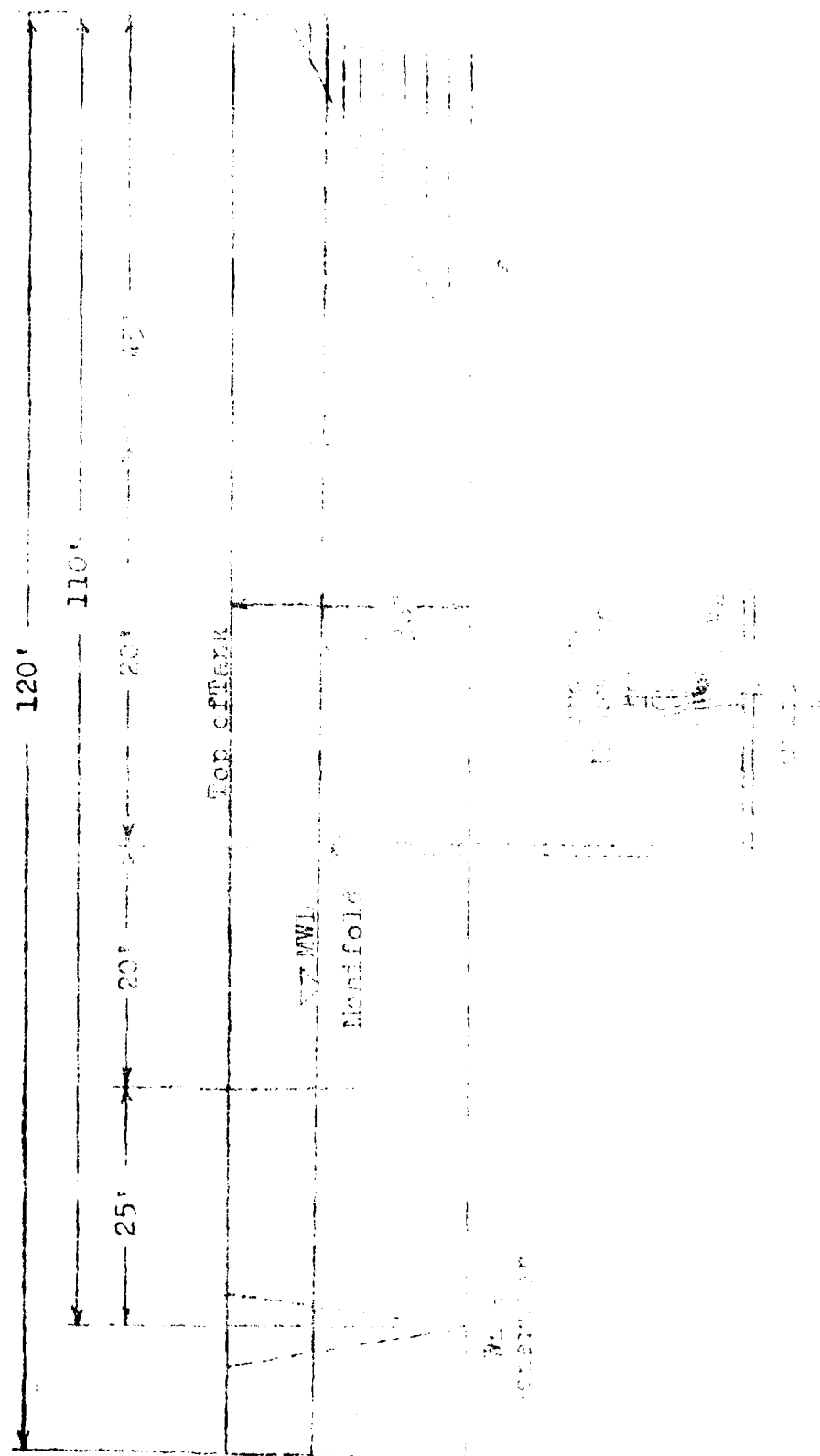
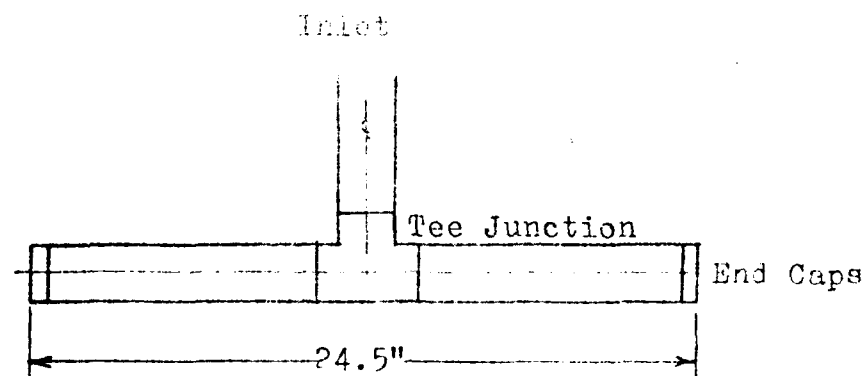


Figure 1. Sample Random Wave Strip Chart



1997, 1998, 1999, 2000, 2001, 2002, 2003, 2004, 2005, 2006, 2007, 2008, 2009, 2010, 2011, 2012, 2013, 2014, 2015, 2016, 2017, 2018, 2019, 2020, 2021, 2022, 2023, 2024, 2025, 2026, 2027, 2028, 2029, 2030, 2031, 2032, 2033, 2034, 2035, 2036, 2037, 2038, 2039, 2040, 2041, 2042, 2043, 2044, 2045, 2046, 2047, 2048, 2049, 2050, 2051, 2052, 2053, 2054, 2055, 2056, 2057, 2058, 2059, 2060, 2061, 2062, 2063, 2064, 2065, 2066, 2067, 2068, 2069, 2070, 2071, 2072, 2073, 2074, 2075, 2076, 2077, 2078, 2079, 2080, 2081, 2082, 2083, 2084, 2085, 2086, 2087, 2088, 2089, 2090, 2091, 2092, 2093, 2094, 2095, 2096, 2097, 2098, 2099, 2100, 2101, 2102, 2103, 2104, 2105, 2106, 2107, 2108, 2109, 2110, 2111, 2112, 2113, 2114, 2115, 2116, 2117, 2118, 2119, 2120, 2121, 2122, 2123, 2124, 2125, 2126, 2127, 2128, 2129, 2130, 2131, 2132, 2133, 2134, 2135, 2136, 2137, 2138, 2139, 2140, 2141, 2142, 2143, 2144, 2145, 2146, 2147, 2148, 2149, 2150, 2151, 2152, 2153, 2154, 2155, 2156, 2157, 2158, 2159, 2160, 2161, 2162, 2163, 2164, 2165, 2166, 2167, 2168, 2169, 2170, 2171, 2172, 2173, 2174, 2175, 2176, 2177, 2178, 2179, 2180, 2181, 2182, 2183, 2184, 2185, 2186, 2187, 2188, 2189, 2190, 2191, 2192, 2193, 2194, 2195, 2196, 2197, 2198, 2199, 2200, 2201, 2202, 2203, 2204, 2205, 2206, 2207, 2208, 2209, 2210, 2211, 2212, 2213, 2214, 2215, 2216, 2217, 2218, 2219, 2220, 2221, 2222, 2223, 2224, 2225, 2226, 2227, 2228, 2229, 2230, 2231, 2232, 2233, 2234, 2235, 2236, 2237, 2238, 2239, 2240, 2241, 2242, 2243, 2244, 2245, 2246, 2247, 2248, 2249, 2250, 2251, 2252, 2253, 2254, 2255, 2256, 2257, 2258, 2259, 2260, 2261, 2262, 2263, 2264, 2265, 2266, 2267, 2268, 2269, 2270, 2271, 2272, 2273, 2274, 2275, 2276, 2277, 2278, 2279, 2280, 2281, 2282, 2283, 2284, 2285, 2286, 2287, 2288, 2289, 2290, 2291, 2292, 2293, 2294, 2295, 2296, 2297, 2298, 2299, 2300, 2301, 2302, 2303, 2304, 2305, 2306, 2307, 2308, 2309, 2310, 2311, 2312, 2313, 2314, 2315, 2316, 2317, 2318, 2319, 2320, 2321, 2322, 2323, 2324, 2325, 2326, 2327, 2328, 2329, 2330, 2331, 2332, 2333, 2334, 2335, 2336, 2337, 2338, 2339, 2340, 2341, 2342, 2343, 2344, 2345, 2346, 2347, 2348, 2349, 2350, 2351, 2352, 2353, 2354, 2355, 2356, 2357, 2358, 2359, 2360, 2361, 2362, 2363, 2364, 2365, 2366, 2367, 2368, 2369, 2370, 2371, 2372, 2373, 2374, 2375, 2376, 2377, 2378, 2379, 2380, 2381, 2382, 2383, 2384, 2385, 2386, 2387, 2388, 2389, 2390, 2391, 2392, 2393, 2394, 2395, 2396, 2397, 2398, 2399, 2400, 2401, 2402, 2403, 2404, 2405, 2406, 2407, 2408, 2409, 2410, 2411, 2412, 2413, 2414, 2415, 2416, 2417, 2418, 2419, 2420, 2421, 2422, 2423, 2424, 2425, 2426, 2427, 2428, 2429, 2430, 2431, 2432, 2433, 2434, 2435, 2436, 2437, 2438, 2439, 2440, 2441, 2442, 2443, 2444, 2445, 2446, 2447, 2448, 2449, 2450, 2451, 2452, 2453, 2454, 2455, 2456, 2457, 2458, 2459, 2460, 2461, 2462, 2463, 2464, 2465, 2466, 2467, 2468, 2469, 2470, 2471, 2472, 2473, 2474, 2475, 2476, 2477, 2478, 2479, 2480, 2481, 2482, 2483, 2484, 2485, 2486, 2487, 2488, 2489, 2490, 2491, 2492, 2493, 2494, 2495, 2496, 2497, 2498, 2499, 2500, 2501, 2502, 2503, 2504, 2505, 2506, 2507, 2508, 2509, 2510, 2511, 2512, 2513, 2514, 2515, 2516, 2517, 2518, 2519, 2520, 2521, 2522, 2523, 2524, 2525, 2526, 2527, 2528, 2529, 2530, 2531, 2532, 2533, 2534, 2535, 2536, 2537, 2538, 2539, 2540, 2541, 2542, 2543, 2544, 2545, 2546, 2547, 2548, 2549, 2550, 2551, 2552, 2553, 2554, 2555, 2556, 2557, 2558, 2559, 2560, 2561, 2562, 2563, 2564, 2565, 2566, 2567, 2568, 2569, 2570, 2571, 2572, 2573, 2574, 2575, 2576, 2577, 2578, 2579, 2580, 2581, 2582, 2583, 2584, 2585, 2586, 2587, 2588, 2589, 2590, 2591, 2592, 2593, 2594, 2595, 2596, 2597, 2598, 2599, 2600, 2601, 2602, 2603, 2604, 2605, 2606, 2607, 2608, 2609, 2610, 2611, 2612, 2613, 2614, 2615, 2616, 2617, 2618, 2619, 2620, 2621, 2622, 2623, 2624, 2625, 2626, 2627, 2628, 2629, 2630, 2631, 2632, 2633, 2634, 2635, 2636, 2637, 2638, 2639, 2640, 2641, 2642, 2643, 2644, 2645, 2646, 2647, 2648, 2649, 2650, 2651, 2652, 2653, 2654, 2655, 2656, 2657, 2658, 2659, 2660, 2661, 2662, 2663, 2664, 2665, 2666, 2667, 2668, 2669, 2670, 2671, 2672, 2673, 2674, 2675, 2676, 2677, 2678, 26





1.5" I.D. PVC with 22  $\frac{7}{32}$ " brass nozzles spaced 1" O.C.

Figure 3. Breakwater Manifold

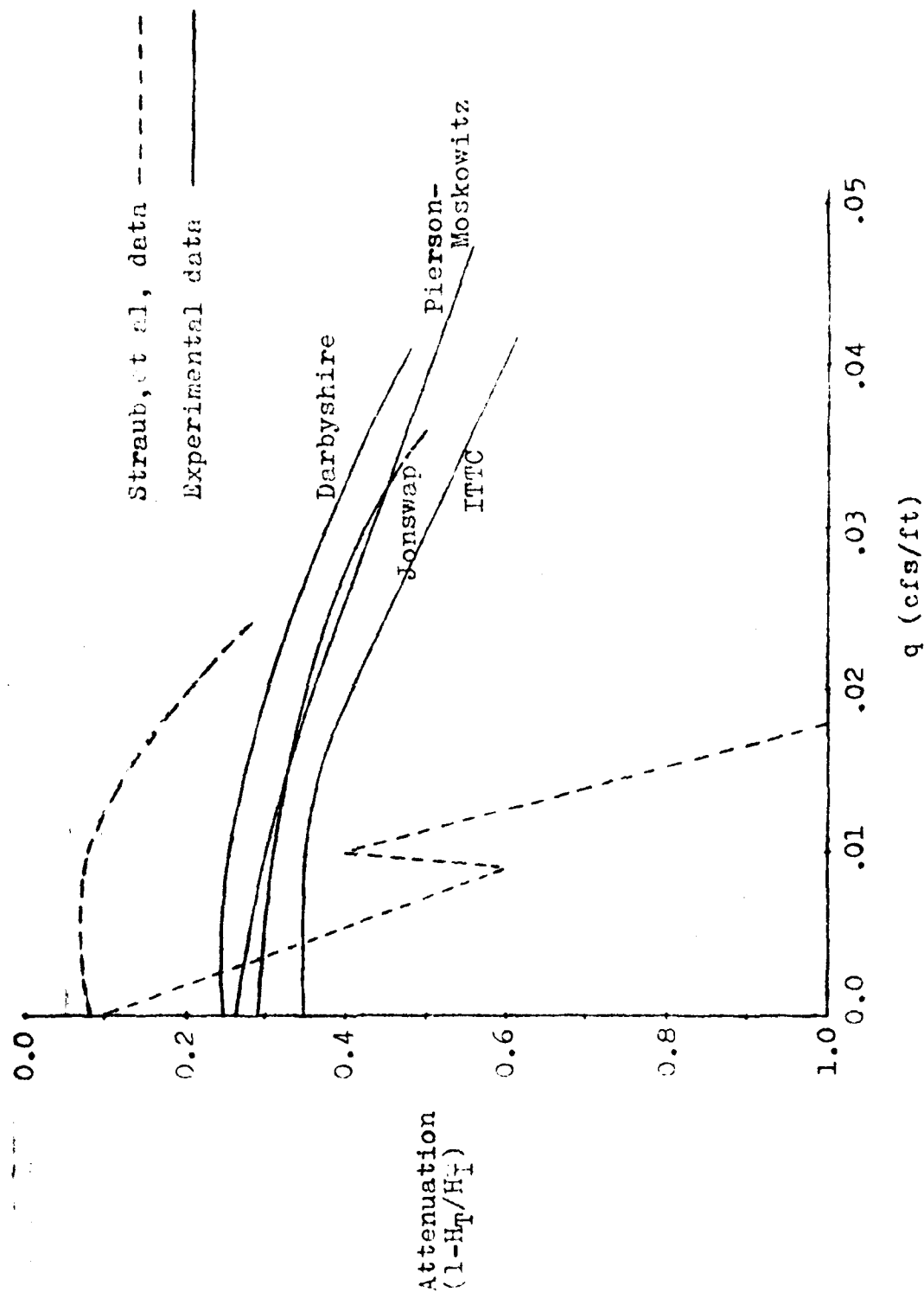


Figure 4. Graph of Attenuation to Unit Discharge for Experimental Results

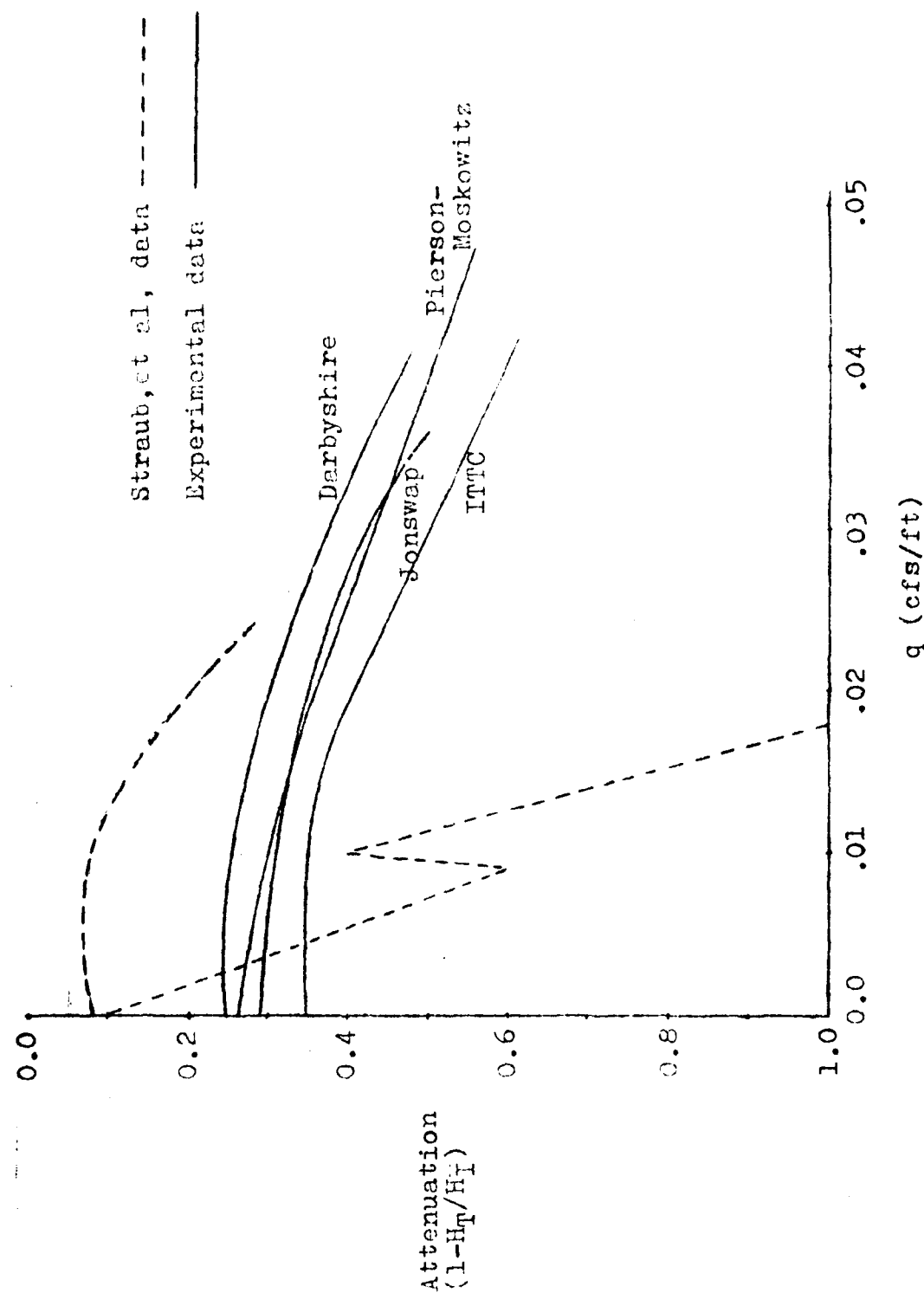


Figure 4. Graph of Attenuation to Unit Discharge for Experimental Results

1. Taylor, G.I. (1955), "The generation of long waves by a cent  
Used in the design of the ... ..  
A, vol. ...
2. Evans, J.W. (1957), "The generation of long waves by a ... ..  
... ..
3. Herbich, J.L. (1960), "The generation of long waves by a ... ..  
... ..  
... ..  
... ..
4. ... ..  
... ..  
Vol. ... ..
5. ... ..  
... ..  
Report ... ..
6. Straub, J.W. (1960), "Experimental investigation of the ... ..  
Breakwaters," University of Minnesota, ... ..  
Falls ... ..  
Series ...
7. Williams, J.A. (1960), "Verification of the ... ..  
... ..  
No. 104-11, ... ..
8. Williams, J.A.; Wiggins, R.L. (1961), "The ... ..  
Wind Waves by ... ..  
on Coastal Engineering, ASCE.
9. Rao, S.V. (1961), "The ... ..  
... ..
10. Hesse, R.W. (1961), "The ... ..  
of ... ..  
... ..  
ASCE, ... ..
11. Albert, R.L. (1962), "The ... ..  
(1959), ... ..  
ASCE, ... ..
12. ... ..  
... ..  
... ..  
No. 744, ... ..

END

FILMED

2-84

DTIC